AlO Bonding: A Method of Joining Oxide Optical Components to Aluminum Coated Substrates

Alexander Coucoulas, Albert M. Benzoni*, Mindaugas F. Dautartas*, Ranjan Dutta, William R. Holland, Casmir R. Nijander and Robert E. Woods

AT&T Bell Laboratories
Princeton, N.J. and *Breiningsville, PA

PUBLICATION DATE: 01.06.93
(further bibliographic data on next page

p.470-481

ABSTRACT

With the increased use of photonic packages, there are needs for reliable and low cost methods of attaching optical components. Packages based on silicon optical bench (SiOB) technology include oxide coated ball-lenses and silica fibers which are generally epoxied in anisotropically etched features of silicon substrates. The reliable attachment of these micro-optical components requires the application of small (approximately 1 nanoliter) quantities of epoxy at precise locations on the substrate. This is a time consuming process and requires considerable operator training and skill. Dispensing too much epoxy can deteriorate the optical performance of the device and dispensing too little results in an insufficient holding power.

AlO bonding is an alternative attachment technique, under development, which forms solid-state bonds directly between these oxide-components and aluminum thin film coated silicon optical bench substrates and therefore does not require the handling of additives, such as epoxy, at the bond interface.

This paper includes: methods of bonding ball-lenses and fibers; an interfacial analysis and proposed bonding mechanism derived from SEM/metallographic photomicrographs and thermodynamic data; destructive test results as a function of bonding and material parameters and; *in situ* loss measurements through AlO bonded components (multi-, single mode fibers and ball-lenses) during the bonding procedures and subsequent thermal cycling (-40 to 80°C and from ambient to -195.8°C) tests.

I. INTRODUCTION

The transition from electronic to optoelectronic and optical packaging has introduced passive transmission components with material properties that are not directly compatible with methods used to join metal conductors in electronic packages.[1] [2] [3] Packages, based on silicon optical bench technology, include silica fibers and oxide ball-lenses which are epoxy bonded in chemically micro-machined V-grooves and pyramidal cavities of silicon substrates. Figure 1 shows these components in position at their permanent sites for the purpose of guiding and collimating optical signals in an optical switch.[4] At present, the reliable attachment of a 300 micron diameter ball-lense requires the application of small quantities (approximately 1 nanoliter) of liquid epoxy in the cavities, positioning the ball in the cavity and holding it in place without rotation while curing the epoxy. This is a time consuming process and requires considerable operator training and skill since it has been found that dispensing too much epoxy can deteriorate the optical performance of the component and dispensing too little results in an insufficient holding power. A similar procedure is used to epoxy fibers in V-grooves.

This paper describes an alternative bonding method which forms solid-state bonds directly between an oxide component and an aluminized silicon substrate and therefore does not require the handling and curing of additives at the bond interface. The objective of this investigation is aimed at bonding oxide coated ball-lenses and silica fibers with the simplicity presently used to join metal conductors in electronic packages. For brevity, the aluminum to oxide bonding technique described herein is referred to as AlO bonding. The report includes an interfacial analysis and mechanical testing of the AlO bonds, and *in situ* loss measurements through various AlO bonded components during the bonding sequence and subsequent thermal cycling tests.

II. MATERIALS

There were three forms of <100> oriented silicon substrates used in this investigation. It included planar substrates; chemically micro-machined substrates with 128 micron wide parallel V-grooves to accommodate fibers, and substrates used in the Silicon-Based Moving Mirror Optical Switch[4] which contain both V-grooves (107 microns wide) and pyramidal cavities. These features are anisotropically etched into <100> oriented silicon wafers using a thermally grown silicon dioxide mask. The oxide mask is removed after etching the features. The etched wafers were sputter-coated with aluminum thicknesses of 1 and 2.5 microns. Optimal adhesion between the sputtered aluminum metal and silicon was achieved by using an *in situ* RF Ar^+ ion beam cleaning, followed by the sputter deposition of the aluminum film in a MRC-603 sputtering machine. The wafers were then diced into appropriate size substrates. Ball-lenses used in this investigation were AR-coated sapphire spheres having a nominal diameter of 300 microns. The anti-reflective coating of silicon dioxide was deposited by chemical vapor deposition, LPCVD, [5] to a thickness of 2240 ± 200 Å. The fibers used in this study were AT&T multimode and single mode fibers having a core/clad diameter of 62.5/125 and 9/125 microns respectively. Relevant material properties of an epoxy used for attaching optical fibers and a commercially pure aluminum is shown in Table I.

III. BONDING PROCEDURE, MECHANICAL TESTING AND EXAMINATION OF BONDED BALLS

In practice, AR coated sapphire ball-lenses and silica fibers are attached to multi-faceted walls of pyramidal cavities and V-grooves in silicon. This multi-point contact strengthens as well as accurately fixes their optical position relative to other attached components. To simplify subsequent destructive testing and interfacial analysis of an AlO bond, the formation of a relatively fragile single area bond will first be described between a 300 micron diameter AR coated sapphire ball and a

0569-5503/93/0000-0470 $3.00 ©1993 IEEE

1993
PROCEEDINGS

43rd ELECTRONIC COMPONENTS & TECHNOLOGY CONFERENCE
June 1-4, 1993

Buena Vista Palace, Orlando Florida

The Electronic Components and Technology (ECTC) is recognized as the premier international forum for presenting the latest developments associated with the design, fabrication and use of electronic materials, devices, components and systems. In the previous 42 years, the conference has demonstrated the ability to produce provocative presentations and discussions concerning the development, manufacturing technology and reliability of a broad spectrum of electronic components and hybrids. This conference is sponsored jointly by the Components, Hybrids and Manufacturing Technology Society of the IEEE and the Electronic Industries Association.

Future dates for ECTC conferences are:

1994 • May 2 - 5
Washington, D.C.

1995 • May 22 -26
Las Vegas, NV

1996 • May 18 - 23
Orlando, FL

Library of Congress Number 78-647174

planar silicon substrate coated with 2.5 microns of aluminum. The AlO bonding of balls in cavities will then be shown.

A. Procedure

A 2.5 micron thick layer of aluminum coated on a planar silicon substrate is positioned over a small vacuum hole of a heated base. The vacuum ensures that the substrate reaches a maximum steady-state temperature for a given temperature setting of the heated base. The ball is then placed on the substrate (Figure 2). After pre-heating the workpieces, a flat-faced metal bonding tool is loaded on the top surface of the ball for a pre-determined time. The inherently low thermal conductivity of the oxide ball and tangential contact that the tool makes on the ball results in an efficient condition for heating the bond region without requiring to heat the tool. If it is necessary, a heated tool could be an effective way to reduce the required base or substrate temperature.

B. Testing

The bonded workpieces were then transferred to the base of a commercial Vertical Bond Tester.[1] A loop-shaped adhesive tape was attached to the jaws of the tester, and then slowly lowered onto the top portion of the ball and stopped before the tape made contact with the surrounding substrate (Figure 3). The tape was then vertically pulled to test the bond. Destructively tested balls conveniently remained tacked to the tape for examination. A lower than maximum pull-strength was usually obtained since most bonded balls were partially peeled during testing. This was confirmed by microscopic observations during testing which showed that the adhesive contact was usually not at precisely the top of the ball.

C. Examination

Figures 4, 5, and 6 show the interface surfaces of a destructively tested pair of workpieces that failed at a pull-force of 8 ±2 gms. The bonding parameters were: pre-heat time≥1 min; bonding temperature= 325°C;[2] load= 600 gms. and; bonding time= 3 sec. Figure 4 shows a top view of the ball tacked to the test-tape and the bond area off-center relative to the circumference of the ball. This view along with observations made during testing substantiated that the majority of bonded balls were partially-peeled during testing, which would result in a lower test value than if it was pulled at a 90 degree angle. For example, balls tested nearer to 90-degrees had recorded strengths of 18 ±2 gms. Balls, bonded on a planar surface and at a single contact spot, have survived an expedient thermal cycling test where the bonded workpieces were immersed in a liquid nitrogen bath (-195.8°C) for about 3 minutes. After the workpieces were removed to ambient conditions, the substrate was tapped on a table and the balls remained bonded.

The substrate workpiece in Figure 5 shows a bond region with three distinct regions. The central region shows a circular-shaped aluminum film which was reduced in cross-section to ≤1 micron in thickness. The film is surrounded by an annular-shaped ring of the underlying silicon where a significant amount of aluminum was removed. Metallographic examination at 1000x shows that the silicon is in-focus with the centrally located aluminum film which was directly below the ball. This indicated the extent of aluminum thinning that took place in this region. The outer annular-shaped ring (shown out of focus) is composed of an extruded aluminum pile. Figure 6 shows an annular-shaped aluminum nugget stuck on the surface of the mating ball having only traces of aluminum in the central region. Its shape shows that it was removed from the substrate in the mid-region where the silicon substrate was exposed (Figure 5). Figure 7 depicts the probable position of a 300 micron diameter ball which penetrated 2.5 microns into an aluminum film. A calculated chordal length which intersects the radius at 2.5 microns is equal to 55 microns. This closely compares to measured[3] outer dimensions of the annular-shaped silicon and aluminum ring shown in Figures 5 and 6 respectively. It is in this mid-region where the surface of the penetrating ball contacts the aluminum as it extrudes outwardedly and forms the outer pile. Fissures are known to develop in an extended native aluminum oxide coatings, as its underlying aluminum is deformed.[6] During AlO bonding, the ball is expected to form contacts with the exposed aluminum at the fissures. Available thermodynamic data[7] in the forms:

$$\Delta G = -RT \ln K$$

and $$\Delta G = A + BT \log T + T$$

where: ΔG= Standard Free Energy

K= Equilibrium Constant

indicates the stable as well as protective nature of the native aluminum oxide coating (equ.-1-) and that exposed areas of aluminum will reform its oxide when exposed to the atmosphere. A reaction is also possible between a silica ball in contact with the underlying aluminum, (equ. -2-) as shown below:

-1- $Al_2O_3 = 2Al + 1.5\ O_2$

ΔG_{25C}= +378 kcal

ΔG_{400C}= +350 kcal

-2- $2Al + 1.5\ SiO_2 = Al_2O_3 + 1.5\ Si$

ΔG_{25C}= -82 kcal

ΔG_{400C}= -79 kcal

The integrity of the bond may further be enhanced with the potential diffusion of silicon in aluminum. The following equilibrium solubilities of Si in Al have been reported: 400°C (0.28 at. %); 350°C (0.16 at %); 300°C (0.10 at %) and; 250°C (0.05 at %).[8]

Less interfacial shear would be expected to take place in the central region as a result of acting frictional forces between the ball and aluminum film. This condition is similar to the onset of plastic flow by a hard indenter compressing a metallic surface which commences just below the surface.[9] During the early stages of film deformation a minimal amount of interfacial flow and therefore sticking just below the ball would be expected as shown in the central bond region (Figures 5 and 6). A further increase in the bonding parameter was observed to increase the extent of adhesion below the center of the ball where the film deformation spreads to the surface.

1. A product of Engineering Technical Products, Inc. 2. Nominal bonding temperatures reported in this report were determined by monitoring a thermocouple with its junction positioned between the tool and substrate. 3. Measurements were made using a Nikon Metallograph and attached UM-2 measurescope.

Figure 8 shows a destructive bond interface on the substrate which was formed at a lower temperature (220°C). Though the bond was too low to pull-test, it revealed a less deformed or indented aluminum film which closely replicated the surface texture of the ball. Examination of balls that were bonded under these conditions showed significantly less sticking of aluminum. The deformation and sticking of the aluminum film at the lower bonding temperatures would be increased by increasing the bonding load or time.

D. Bonded Balls In Cavities

As previously noted, balls bonded in pyramidal cavities accurately fix their optical position as well as form multi-point contacts for added strength. Figure 9 show balls that were bonded in a cavity of a 2.5 micron thick aluminum film on a silicon substrate. It was found that these bonded balls could not be destructively tested, as previously described, since the adhesive repeatedly failed leaving the ball intact. The repeated stressing of AlO bonds as the adhesive failed on the same bonded ball was typically 16 ±2 gms. In order to examine the bond interfaces, the ball was pushed out of the cavity with a probe. Figures 10 and 11 show the dislodged ball and the cavity respectively. Figure 12 shows a higher magnification of a bond region on the silicon wall. It shows a greater amount of aluminum piled in the lower contact region which implies that a downward-shearing motion between the ball and the aluminum occurs during bonding. The additional interfacial shear that occurs against the angular wall of the cavity would be expected to enhance the integrity of the bond compared to forming it on a planar surface as previously described. Figures 11 and 12 also show that more aluminum remained where the ball made its closest contact with the silicon wall as the underlying aluminum extruded outward. Energy Dispersive X-Ray (EDX) analysis indicated that there was residual aluminum throughout the bond area on the silicon wall with a higher percentage localized in the off-center region (Figure 12). Figure 12 and a higher magnification (Figure 13) of the aluminum stuck on the ball also indicated that the aluminum was reduced to ≤0.25 micron where the ball made its closest contact with the silicon wall. This was similar to what was found when the ball was bonded to the planar surface previously described. Figure 14 shows the aluminum deposit on the surface of the ball. Its shape clearly shows that it was removed from the silicon wall (Figure 12) as well as showing where the spot of closest contact occurred. AlO bonded balls have also been pushed off with a probe tester positioned parallel to the aluminized (2.5 microns) silicon surface resulting in typical values of 35 ±3 gms. These values were also obtained after pre-stressing the bond with the vertical tester as described above.

IV. MECHANICAL SHOCK AND VIBRATION TESTING OF ALO BONDED BALL-LENSES

AlO bonded balls were prepared for shock and vibration testing. Six silicon substrates containing four pyramidal cavities were coated with 2.5 microns of aluminum. Four AR-coated ball-lenses were bonded in each of six substrates. Two aluminum alloy test carriers were used to secure the substrates. Three substrates were epoxied to the face of each carrier. The test carriers, each containing 12 AlO bonded lenses, were then subjected to shocks up to 2000G's (0.5 ms) on all axes and 20G vibration levels from 10 Hz to 2 KHz on all axes. All 24 bonded lenses remained bonded under these test conditions resulting in a 100% yield. The test levels used in this run met or exceeded military specifications for mechanical integrity. Figures 15 and 16 show one of the test carriers after completing the shock and vibration tests.

V. AlO BONDING SILICA FIBERS

Epoxy bonding fibers in V-grooves of silicon substrates which contain previously AlO bonded ball-lenses in neighboring aluminized cavities may now be considered feasible. This is a result of the high temperature properties of an AlO bond and the ability to localize or pattern generate the deposited aluminum film. Since the bare fiber is composed of silica, the next phase of this investigation explored a method to AlO bond fibers and test their mechanical properties as a function of the bonding and material parameters.

A. Fiber Preparation

Four-inch lengths of polymer coated fibers were mechanically stripped (about 0.5 inches) at one end. Next, the ends were wiped several times with a methyl alcohol soaked tissue (to remove the residual coating) and then wiped dry.

B. Bonding Fibers

A silicon substrate with 128 micron wide parallel V-grooves and coated with 2.5 microns of aluminum was fixed by vacuum to the heated base of the bonder. After pre-heating the substrate, the stripped end of the fiber was positioned in a V-groove and held until a flat faced bonding tool was loaded on the fiber for a given time. The end of the fiber extended beyond the tool to ensure reasonable consistency in the bonded length. The bonded fiber would therefore tail-in and out of the aluminum film which would not necessarily result in the maximum strength for a given bond length since a slight peel action rather than a complete shear test was expected to occur. Deposited aluminum lands or pads of a given dimension would of course negate this concern and define the bond length. It should be noted that the polymer coated section of the fiber was prevented from reaching its depolymerization temperatures during bonding.

Figure 17 and 18 show regions of two bonded fibers where the tool made contact during bonding. Figure 17 shc residual polymer which remained on the surface of the fibe. Figures 18 and 19 show smooth surfaces of bonded fibers with no traces of the residual polymer due to a thorough pre-cleaning step prior to bonding. In practice, the unbonded portion of the fiber (shown in Figure 19) could be secured and relieved of mechanical stresses by cementing or securing it in the V-grooved substrate where the polymer coating begins.

C. Test Procedure

A substrate with a bonded fiber was clamped on a horizontal stage of a commercial pull tester (Figure 20). The free end of the fiber was then carefully z-positioned on a hard wax surface which was predeposited on a metal tab clamped to the pull-rod of the testing machine. The wax was momentarily heat-softened to wet and stick the fiber to the metal tab for pull-testing. The fiber was then pulled approximately parallel to its axial length until a destructive failure occurred. The final pull-strength and the mode of failure was recorded.

D. Test Results

Individual Pull Strengths vs. Temperature along with the bonding conditions are shown in Figure 21. All the failure modes of the plotted data points showed that the fiber remained intact and that aluminum was stuck to their surfaces. The pull strengths are shown to increase with the bonding temperature. This would be expected since the flow properties of aluminum decrease with temperature which would result in an increase in the real contact or bonded area. Figure 21 shows that pull-strengths near one pound (454 gms) can be obtained at a bonding temperature of 300°C. Temperatures below 225°C produced strengths too low to test using the bonding parameters indicated in Figure 21. A sample (five) of bonded fibers were put in a temperature/humidity chamber (120°C/85%) for 100 hours and pull tested. All the tested fibers remained in tact with strengths similar to those shown in Figure 21.

Figure 22 shows additional data points corresponding to a shorter bonding time of 3 seconds. At the lower temperatures, an increase in the bonding time appears to have more of an effect on increasing the pull-strength than at the higher temperatures. This could be explained by the inherent decrease in flow properties (or increase in rate of aluminum deformation) and strain hardening index of aluminum with temperature.

Figure 23 shows the same plot as in Figure 16 with the addition of data points corresponding to a lower bonding force of 500 gms. The data shows a lowering in the pull strength for a given temperature compared to the points corresponding to the higher bonding force of 1200 gms. Again this could be explained by the flow properties of aluminum. Higher forces would be expected to produce higher strengths until the fiber bottoms-out near the silicon surface or one of the workpieces crack.

Figure 24 shows the addition of a datapoint corresponding to a pull-strength of 715 gms. (~1.6 lbs) where the destructively tested fiber remained in-tact. This was obtained with a longer flat-faced bonding tool and indicates the effect of bond length on the final pull strengths.

Figure 25 shows an aluminized silicon substrate where two bonded fibers of different bond lengths were pull-tested. The remaining fibers were left intact. Strengths of 513 gms and 322 gms. were obtained with values that were approximately proportional to their bond lengths. In this case a closer correlation could not be made since the same forces and therefore different interfacial pressures were actually applied. The average nominal pull-strength in shear for these two fibers was approximately 11,700 psi which was determined from the dimensions of the indentation in the film. This value closely compares to reported shear strengths of aluminum at room temperature (Table I). A closer determination would require a measure of the true contact area. Figure 26 shows one side of a pulled fiber with two parallel bands of heavier aluminum stuck on one side of a pulled fiber which was transferred from one side of the angular wall (Figure 27). This condition was also observed on the other side of the fiber and wall. Less aluminum was found where the fiber made its closest contact with the angular silicon wall. This condition was similar to bond regions examined below bonded balls on planar surfaces and on angular walls of a cavities as previously described. A closer examination of the bond regions showed deformed and sheared aluminum. This further indicated that the controlling strength mechanism of fibers pulled parallel to their axial length is the shear strength of aluminum.

Figure 28 shows a plot of Pull-Strength vs. Aluminum Thickness. It shows that there is an increase in the strength with aluminum thickness. This could be explained by an increase in the final bond area.

IV. OPTICAL LOSS MEASUREMENTS

We will now describe *in situ* loss measurements through AlO bonded components which will be subjected to the handling and bonding procedures previously described. Measurements will be made through the following bonded components: (1) a fiber bonded on a planar surface and in a V-groove; (2) a set of spliced fibers bonded in a V-groove and: (3) two fibers and two intervening ball-lenses bonded in-line on substrates used in the 2x2 Silicon-Based Moving Mirror Optical switch package (Figure 1). *In-situ* loss measurements of bonded components during various thermal cycling procedures were also made.

A. Measurement Procedure

The majority of measurements through the bonded components utilized three meter lengths of AT&T multi-mode and single mode fibers connected between an LED source (1300 nm) and power meter. The accuracy of the reported losses were ±0.01 dB, unless it was otherwise stated. The fibers were wrapped five times around a 1/2-inch diameter teflon rod near the input end to achieve mode mixing and the resultant stabilized output intensity signal was recorded. The losses (α) were calculated by measuring the output intensity before (I_o) and after (I_f) forming the bonded components.

$$\alpha = -10\text{Log}\,(I_f / I_o)$$

B. Thru Bonded Fibers

The center section (≈10 cm) of a 3 meter length of multi-mode fiber was stripped of its polymer coating and cleaned. The ends were then connected to a 1300 nm LED source and power meter. The stablized output signal was then recorded. A 2.5 micron thick layer of aluminum coated on a planar silicon substrate was fixed by vacuum to the heated base of the bonder. After the substrate was preheated (≥1 min), the bare portion of the fiber was positioned on the substrate. The bonding tool (35 mil square) was then loaded (1400 gms) on the fiber for 13 sec. at a bonding temperature of 298°C. The bonded workpieces were then removed and cooled to ambient temperatures. The intensity of the output signal remained constant (loss= 0.00 dB) throughout each sequence from bonding at 298°C to ambient. A similar bonding and *in situ* loss measurement experiment was made with the addition of an expedient thermal cycling test. The bonded workpieces were held by their extending fibers "jump-rope-style" in order to immerse it in a liquid nitrogen bath (-195.8°C) for about 3 min. The output signal indicated no change for each of the three cycles. The same results were obtained by temperature cycling (three times) a bonded fiber from a liquid water bath at 0°C to ambient.

C. Spliced Fibers

A three meter length of a single-mode fiber was connected to a 1300 nm LED source and power meter. After the output signal was recorded, the fiber was cut in half. The polymer coating of the fiber was stripped and cleaned along approximately 1 inch of each cut end. The ends were then cleaved with a hand held tool and cleaned again. An aluminum thin film (2.5 micron thick) coated silicon substrate, with 128 micron wide V-grooves, was fixed by vacuum to the heated base of the bonder. After pre-heating the substrate for ≥1 minute, a fiber end was positioned in a V-groove and held until the tool was loaded on the fiber at a temperature of 298°C. The face of the tool was allowed to extend approximately 10 mils beyond the end of the fiber. The second fiber-end was butted against the bonded fiber and compressed by the tool. The face of the tool was again positioned so that it extended about 10 mils beyond the end of the previously bonded fiber. During the second bonding cycle, the power meter registered an increase in the output signal. There was no change in the intensity as the bonded splice was removed from the heated base to ambient. A set of five typical splices with an index matching gel in place resulted in an average loss= 0.09 dB with a range from 0.05 to 0.20 dB.

Three of the above bonded splices underwent thermal cycling in a liquid nitrogen bath (195.8°C) as previously described. The average additional room temperature change in loss after the combined nine cycles was 0.01 dB. Also, there were no detectable losses monitored from room to liquid nitrogen temperatures in each of the nine cycles. After the cycling tests were complete, the extending fibers of one splice, used in these experiments were pull-tested with resultant strengths of 336 gm. (bond length= 0.037-inch) and 241 gm. (bond length= 0.027-inch). Both pull-tested fibers remained intact with aluminum deposited on their surfaces.

An earlier AlO bonded splice was mounted by taping the extending fibers to a glass slide. The mounted splice was then held "jump-rope style" by the extending fibers for immersion in a liquid nitrogen bath. During the immersion cycle the glass slide shattered while the attached splice remained intact and continued to transmit the intensity signal with no detectable loss. The quenching cycle was repeated two more times by holding the extending fibers for the immersion step. No loss or change in signal was detected at room temperature as a result of the three quenching cycles. Earlier thermal cycling (-80 and 40°C) of fibers spliced in a V-groove resulted in no change in loss at room temperature after 33 cycles at which time the coolant was exhausted. Similar results were obtained with splices cycled in boiling water (33 min) and in ice-water (33 min). In these early experiments multi-mode fibers were connected between an 850 nm LED source and a battery-operated power meter (0.1 dBm resolution). Figure 29 shows an SEM photomicrograph of a spliced fiber bonded in a V-groove. Figures 30 and 31 show a fiber bonded at its end by overlapping the tool and its penetration into a 2.5 micron thick aluminum.

D. In-Line Bonded Fibers and Ball-Lenses

Two 300 micron diameter balls were placed into two in-line cavities of an aluminized silicon switch-base and bonded (Figure 1). A three meter length of a multi-mode fiber was connected to a 1300 nm LED source and power meter. Two fiber ends were prepared and connected to the loss-measurement set-up as previously described and bonded into the V-grooves behind each bonded ball (Figure 32 and 33.). During bonding of the second fiber, an output signal was detected. As in the case of splices, previously described, the output signal did not change while it was transferred from the heated base to room temperature. A sample of four in-line bonded substrates with an index matching gel deposited between each fiber and ball resulted in an average straight thru loss= 0.49 dB with a range between 0.40 and 0.58 dB. The maximum allowable and average loss for a straight thru connection are 1.1 and 0.7 dB respectively.[4] *In situ* measurements of three samples were made by holding their extending fibers and cycling three times between liquid nitrogen and room temperature resulting in no change in loss at R.T. There were also no losses shown from room temperature to liquid nitrogen temperatures in each cycle while the bonded sample was immersed in liquid nitrogen.

V. Summary

This paper has described and characterized a method which permanently bonds oxide coated ball lenses and silica fibers to aluminized silicon substrates with the use of heat and pressure. The method of forming the aluminum to oxide bond is referred to as AlO bonding . Its objective is aimed at solid state bonding optical components in packages with the simplicity of joining metal conductors in electronic packages. The resultant data was obtained after subjecting the components to handling procedures typically required during their preparation and subsequent bonding which is expected to be representative of manufacturing conditions. The following is a summary of the work:

1. The aluminum to oxide bond occurs as a result of interfacial shear and contact between the silica component and aluminum where it is exposed at fissures of its extended native oxide protective coating. Thermodynamic data was presented to show that the reaction was possible. It was also shown that aluminum was stuck to the destructively tested oxide component.

2. A means of pull testing bonded balls and fibers were developed. Typical values of 35±3 gms resulted when bonded balls are pushed out of aluminized (2.5 micron thick) micro-machined cavities with a probe testing machine positioned parallel to the silicon substrate.

3. AlO bonded balls were also shock and vibration tested at levels that met or exceeded military specifications for mechanical integrity and resulted in 100% yield.

5. Fibers bonded to aluminized V-grooves were pulled parallel to their axial length. Pull-strengths were shown to increase with an increase in the bonding parameters, the thickness of the aluminum film and longer bond lengths. Typical pull-strengths near one pound (454 gms.) were obtained when using bonding temperatures of 300°C. All the the individual pull-strengths values reported in this investigation resulted in the tested fiber remaining intact. This included a sample of bonded fibers that were pulled tested after aging for 100 hours in a temperature/humidity (120°C/85%) chamber.

6. *In situ* loss measurements (with an accuracy of ±0.01 dB) were made during the formation of AlO bonded

components through: a bonded fiber; a pair of fibers bonded and spliced in a V-groove and; two fibers and two intervening ball-lenses bonded in-line into etched V-grooves and cavities. No loss was observed through bonded fibers. These results were shown through each sequence from bonding at 298°C to ambient. Similar results were observed during thermal cycling from liquid nitrogen to room temperature and, ice water to ambient. Typical single-mode splice losses resulted in an average loss= 0.09 dB. Splices that were immersed in liquid nitrogen and removed to ambient resulted in an average change in loss of 0.01dB at ambient. The average straight through loss measurements between two bonded fibers and two intervening bonded ball-lenses were equal to 0.49dB with a range between 0.40 and 0.58 dB. This was well within an allowable value of 1.1 dB for a reported optical switch[4] which used the same type of chemically micro-machined substrate.

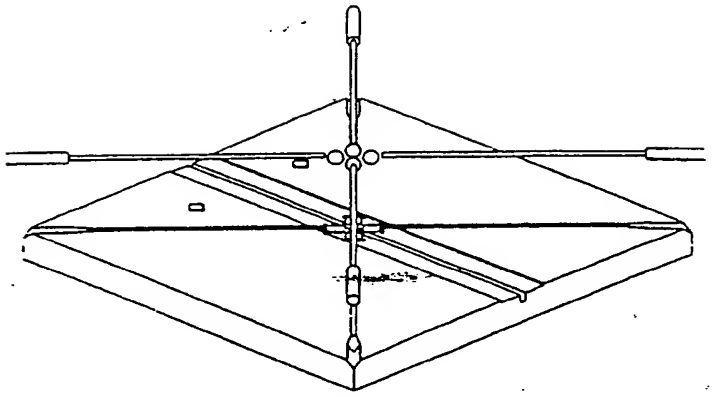

Figure 1. Assembly view of a chemically micro-machined silicon substrate

TABLE 1 - Relevant Properties of a High Temperature Epoxy[1] And Commercially Pure Aluminum[2]

EPOXY	
Number of Components	2
A Cure Schedule	150 °C for 10 min.
Lap Shear Strength	1100 psi
Glass Transition Temp.	130 °C
Coef. of Thermal Exp.(<130 °C)	49×10^{-6} in./in./°C
Coef. of Thermal Exp.(>130 °C)	165×10^{-6} in./in./°C
Outgas to 300 °C	0.31%
Shelf Life	One Year At Room Temp.
ALUMINUM	
Shear Strength	10,000 psi
Tensile Strength (25 °C)	13,000 psi
Tensile Strength (400 °C)	7,500 psi
Melting Point	660 °C
Coef. of Thermal Exp. (-60 to 20 °C)	23.7×10^{-6} in./in./°C
Coef. of Thermal Exp. (20 to 300 °C)	25.6×10^{-6} in./in./°C

1. Epoxy Technology Inc.
2. ASM Metals Handbook, 1948.

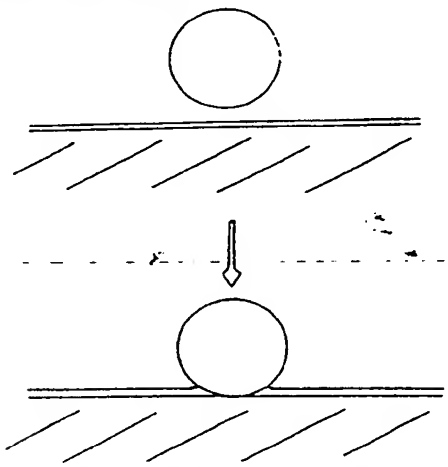

Figure 2. Schematic cross-section of an oxide coated ball-lens and flat aluminized silicon substrate prior to (a) and during (b) AlO-bonding.

ACKNOWLEDGEMENTS

The authors would like to thank their colleagues for their assistance during this investigation: R. Borutta, J. G. Cavalli, L. E. Fanucci, R. E. Frazee, J. P. Honore, S. A. Gahr, B. H. Johnson D. M. Ors, R. F. Roberts, C. M. Schroeder, D. R. Smithgall, L. S. Watkins, K. L. Komarek and M.A.C.

REFERENCES

1. Conti, R.J., "Thermocompression Joining Techniques for Electronic Devices and Interconnects," Metals Engineering Quarterly, vol. 6, pp. 29-35, 1966.

2. Peterson, J.M., H.L. McKaig, and C.F. DePrisco, "Ultrasonic Welding in Electronic Devices," IRE International Convention Record, vol. 10, pp. 3-12, 1962.

3. Coucoulas, A., "Hot Work Ultrasonic Bonding (Thermosonics)," Proceedings Electronic Components Conference, pp. 539-556, 1970.

4. Dautartas, M.F., A.M. Benzoni, Y.C. Chen, G.E. Blonder, B.H. Johnson, C.R. Paola, E. Rice, and Y.-H. Wong, "A Silicon-Based Moving-Mirror Optical Switch," Journal Of Lightwave Technology, vol. 10, no. 8, pp. 1078-1085, 1992.

5. Smolinsky, G. and R.E. Dean, "LPCVD Oxide Films In The Temperature Range 410 to 600°C from Diacetoxyditertirarybutoxysilane," Materials Letters, vol. 4(5-7), pp 256-260 (1986).

6. Metals Handbook, ASM, 1948 ed.

7. Kubaschewski, O, and Evan, E. LL., "Metallurgical Thermochemistry", Pergamon Press, 1958.

8. Hansen, M., "Constitution of Binary Alloys," McGraw-Hill Book Co, Inc., 1958.

9. Tabor, D., "The Hardness of Metals", Oxford Univ. Press, N.Y., 1951.

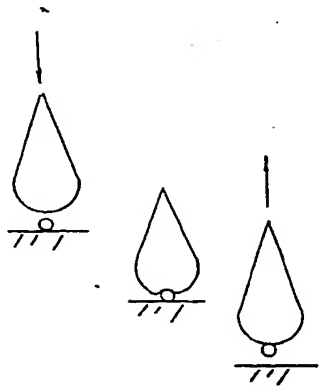

Figure 3. Schematic views of the destructive test procedure. A looped-taped is first lowered to the top surface of a bonded ball for tacking and subsequent pull testing.

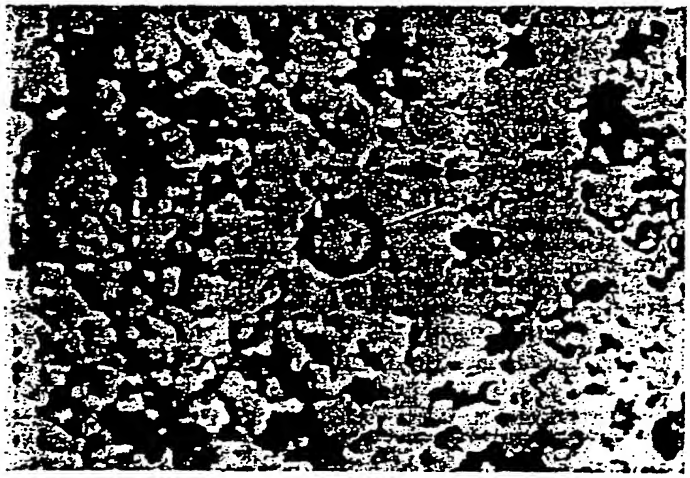

Figure 4. Top view of a destructively tested ball attached to an adhesive tape shown in the surrounding background. Note the bond region (as indcated) is off-center relative to the circumference of the ball. 50x (reduced 25% for printing)

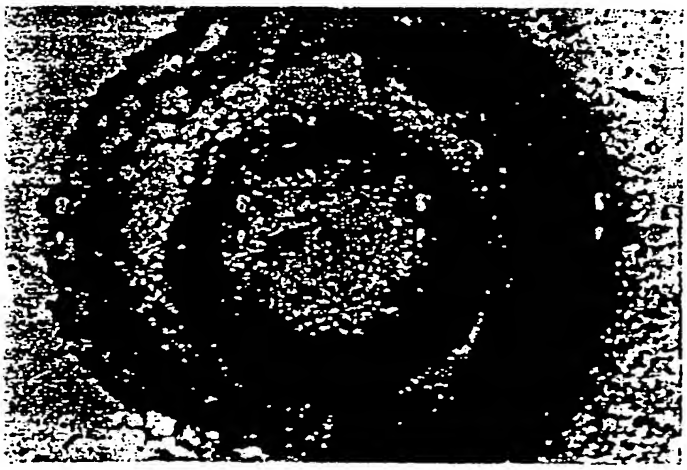

Figure 5. Top view of the aluminum thin film coated silicon substate showing the following three distinct regions: an inner circular region of thinned aluminum: a partial annular-shaped ring of underlying silicon and; an outer ring of an aluminum pile shown out of focus. 1000x (reduced 25% for printing).

Figure 6. Top view of a partial annular-shaped aluminum nugget stuck on the surface of the tested ball. 400x (reduced 25% for printing).

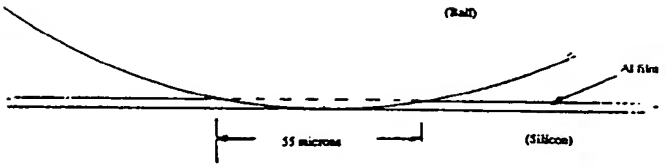

Figure 7. Schematic of a 300 micron diameter ball penetrating a 2.5 microns aluminum thin film on silicon showing its chordal length (55 microns) in-line with the surface of the film.

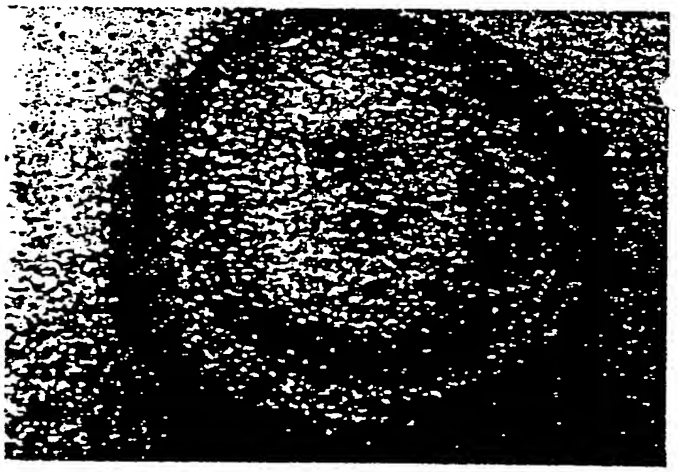

Figure 8. Top view of an aluminum thin film coated silicon substrate showing textural indentation that replicates the surface of the ball. 1000x (reduced 25% for printing).

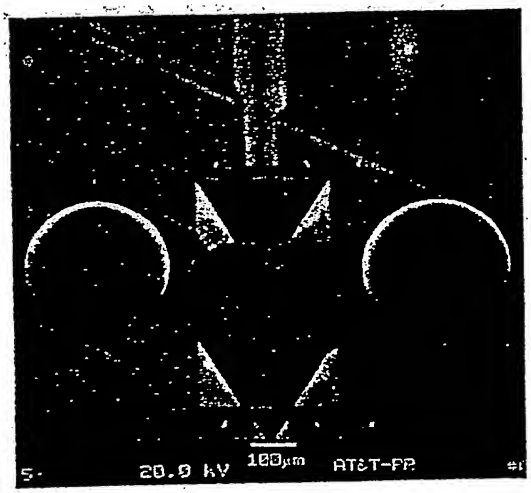

Figure 9. AlO bonded ball-lenses. Bonding parameters were: temp= 298°C: pre-heat≥ 1 min.; load= 600 gms. and; bond time= 13 sec.

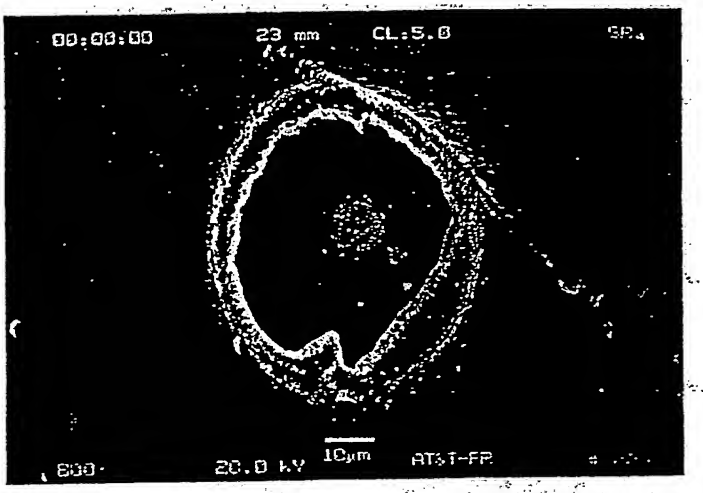

Figure 12. Bond region on the cavity wall showing a high concentration of aluminum remaining in the off-center region.

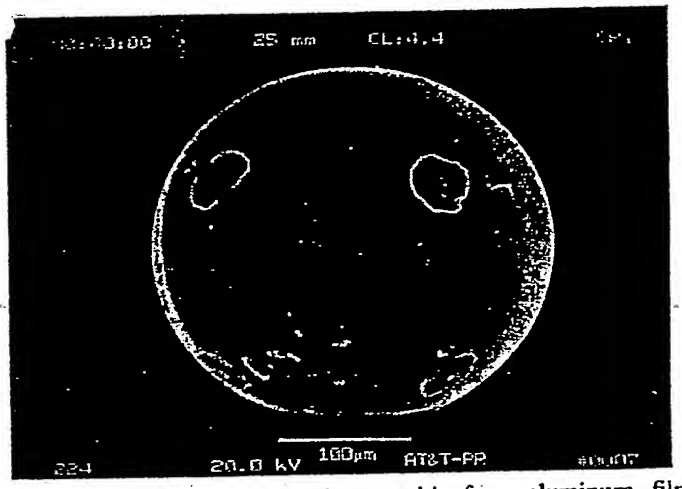

Figure 10. Dislodged ball-lense with four aluminum film sections stuck to its surface.

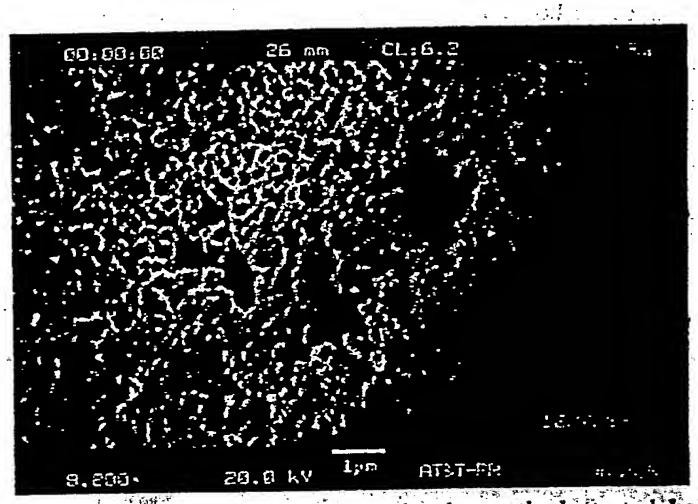

Figure 13. Aluminum deposit on the destructively tested ball showing the thinned topographical features in the vicinity where the ball made the closest contact with the silicon wall (upper left).

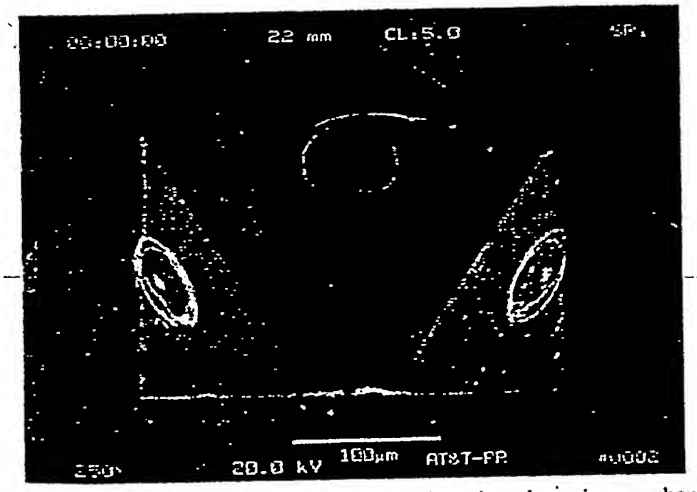

Figure 11. Pyramidal cavity showing bond regions where aluminum was removed during push-testing of the bonded ball shown in Figure 10.

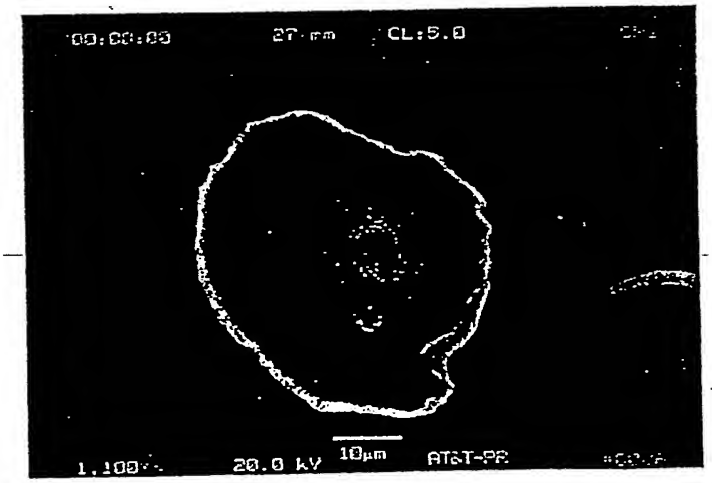

Figure 14. Aluminum deposit stuck on the destructively tested ball which was pushed out of the cavity shown in Figure 12.

Figure 15. Aluminum test carrier with three attached substrates with all 12 bonded balls remaining in the cavities after shock and vibration testing.

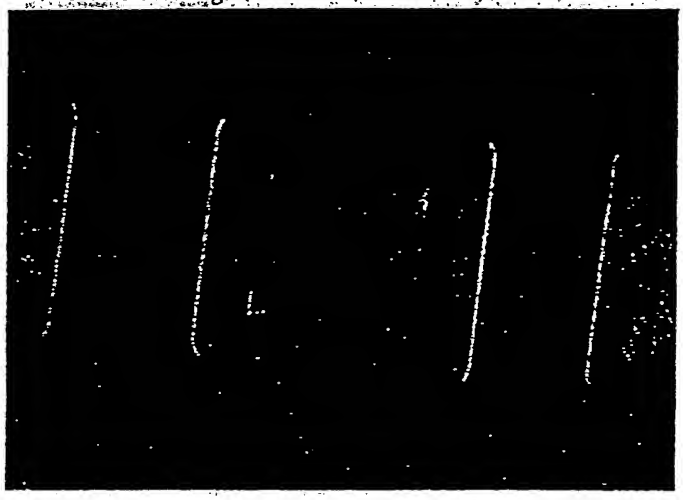

Figure 16. One of the three substrates attached to the aluminum test carrier with all 4 bonded balls remaining after shock and vibration testing.

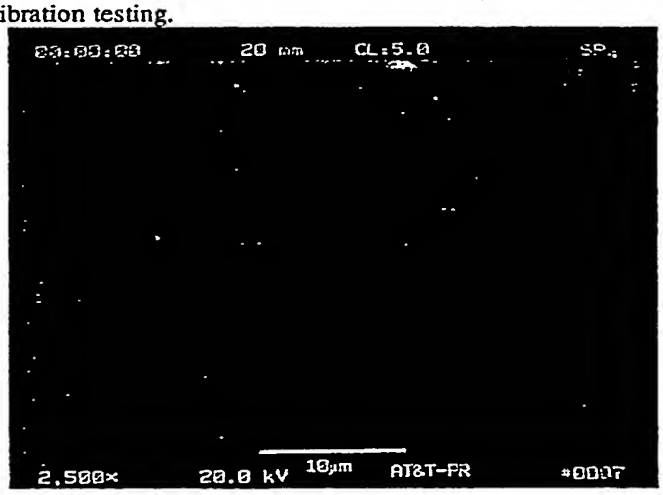

Figure 17. Top view of a bonded fiber in an aluminized V-groove showing islands of the remaining polymer coating.

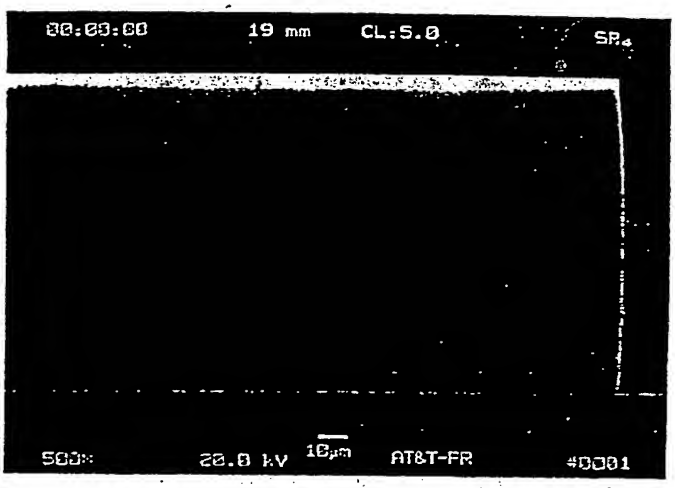

Figure 18. Top view of a fiber-end in the region where the tool made contact during the bonding cycle. Its cleaned surface shows no evidence of the residual polymer.

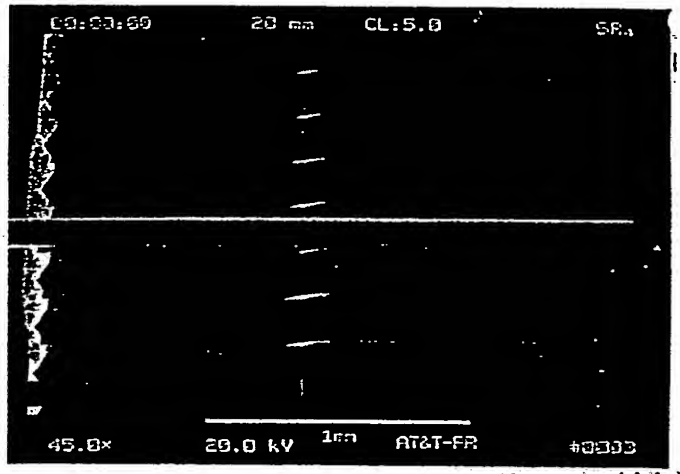

Figure 19. Top view of a bonded fiber in a V-groove (right) and the extending free end (left).

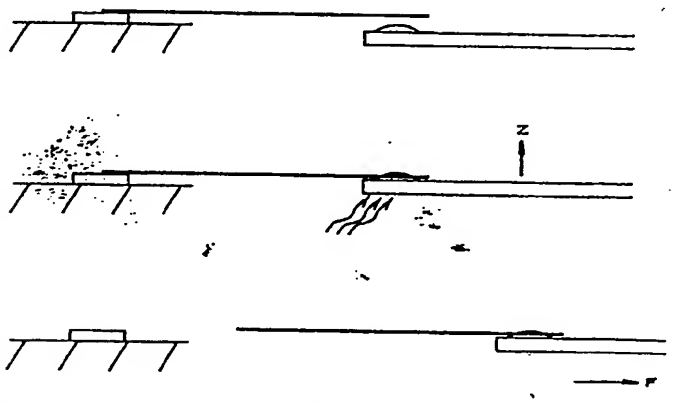

Figure 20. Schematic of the fiber pull-testing procedure showing: positioning of the fiber end to the waxed pull-rod of the testing machine; the wax sealing of the fiber end and; the destructive pull tested fiber remaining in-tact.

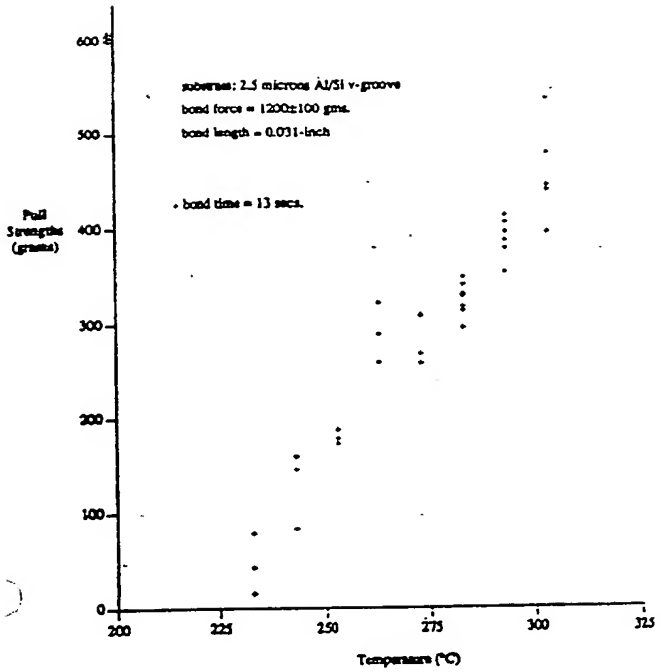

Figure 21. Individual Pull Strengths vs. Temperature for a set of bonding parameters.

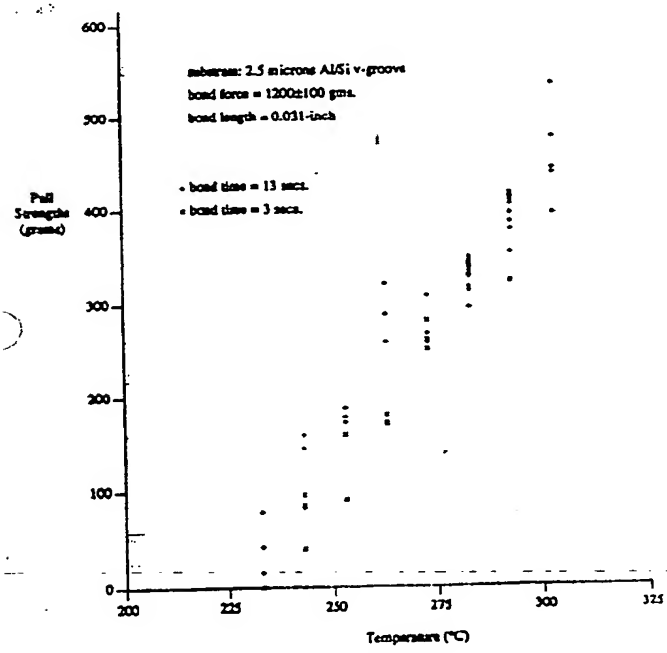

Figure 22. Individual Pull-Strengths vs. Temperature for two sets of bonding parameters having different bonding times.

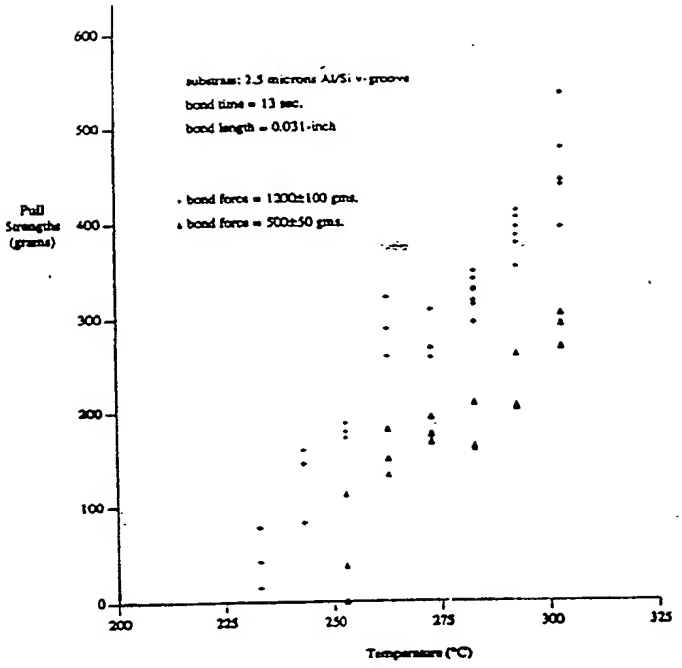

Figure 23. Individual Pull-Strengths vs. Temperature for two sets of bonding parameters having different bonding forces.

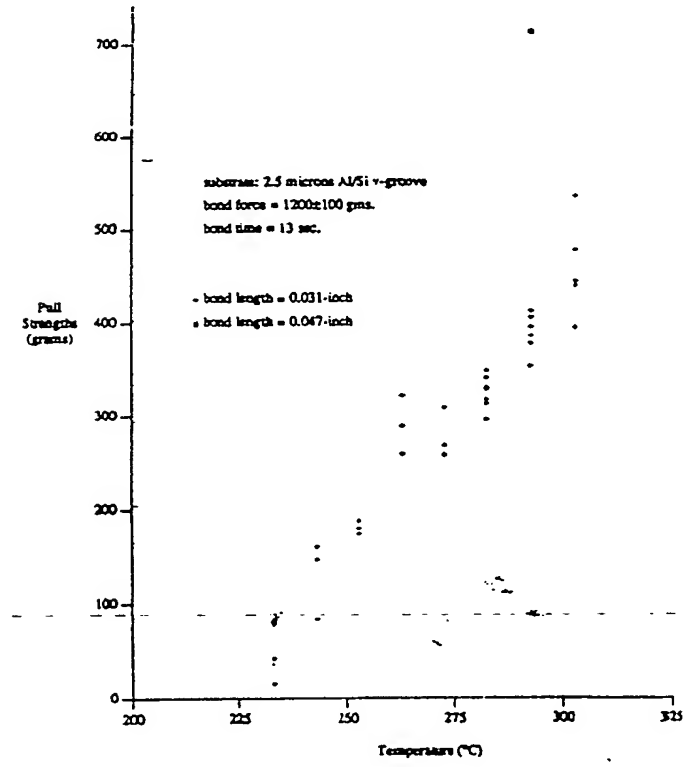

Figure 24. Individual Pull-Strengths vs. Temperature for bonding parameters having different bond lengths.

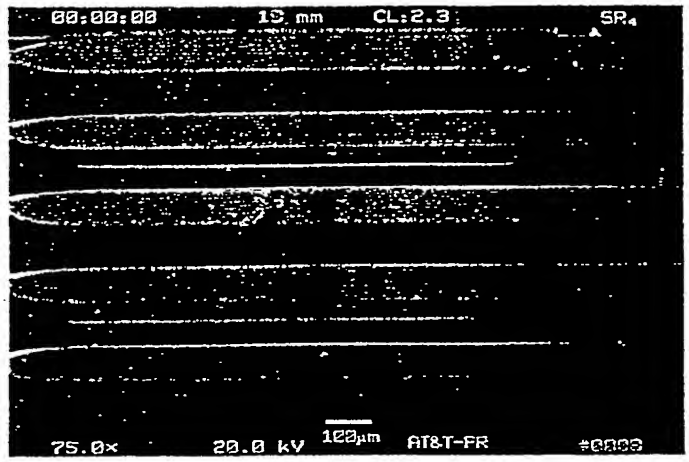

Figure 25. Top view of a substrate with parallel V-grooves showing one side of two bond regions of different lengths where the fibers was a pull-tested in shear with resultant strengths of 322 gms (upper bond region) and 513 gms (lower bond region). Both destructively tested fiber remained in-tact with aluminum stuck to their surfaces.

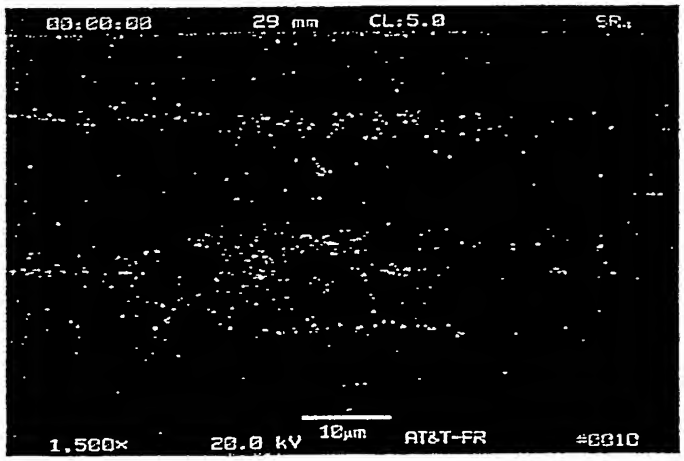

Figure 26. The bond region of a pull-tested fiber which was in-tact after testing. It shows two parallel bands of aluminum which was removed from one side of the V-groove.

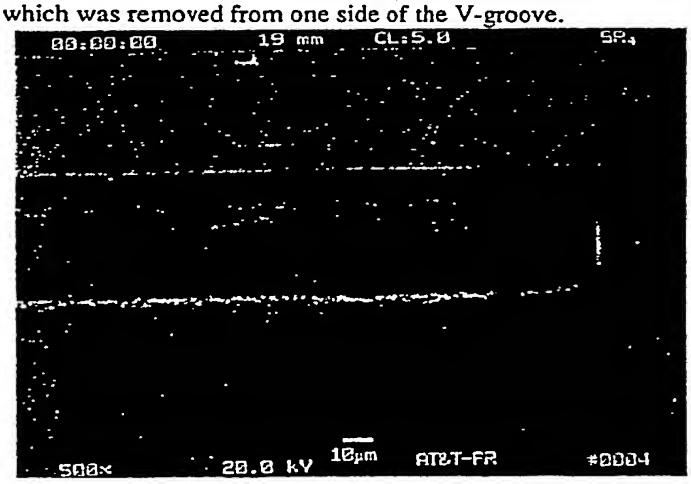

Figure 27. Bond region from one side of the V-groove where a bonded fiber was pull tested. A similar bond region was observed on the opposite angular wall.

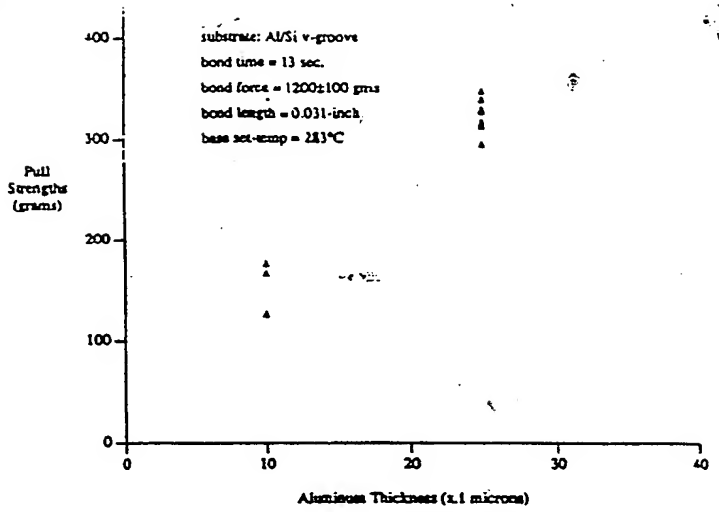

Figure 28. Individual Pull-Strengths vs Aluminum Thickness

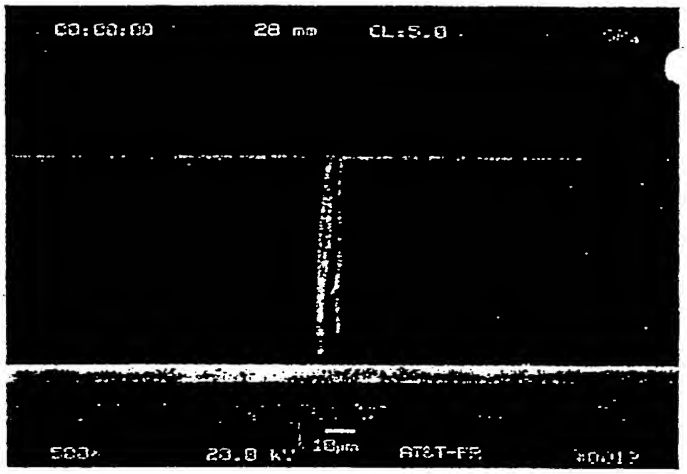

Figure 29. Side view of spliced fibers without index matching gel in place. Top portion of the splice shows the relative z-position of the fibers.

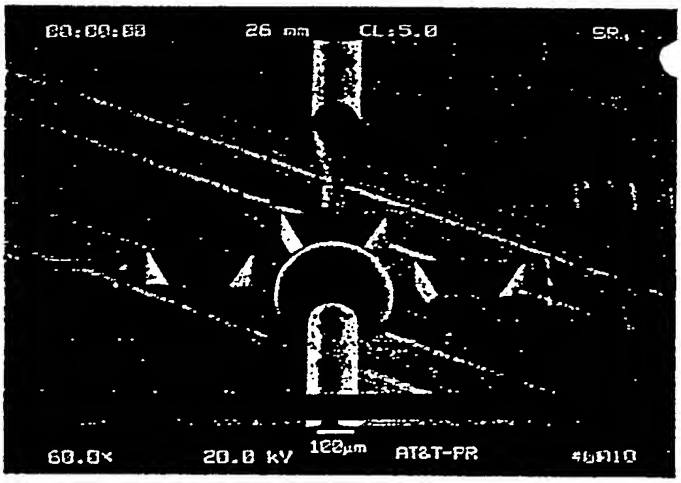

Figure 30. Fibers and a ball lense bonded to an optical silicon base. Lower bonded fiber was bonded at the required position. The upper fiber was bonded out of position to view its end.

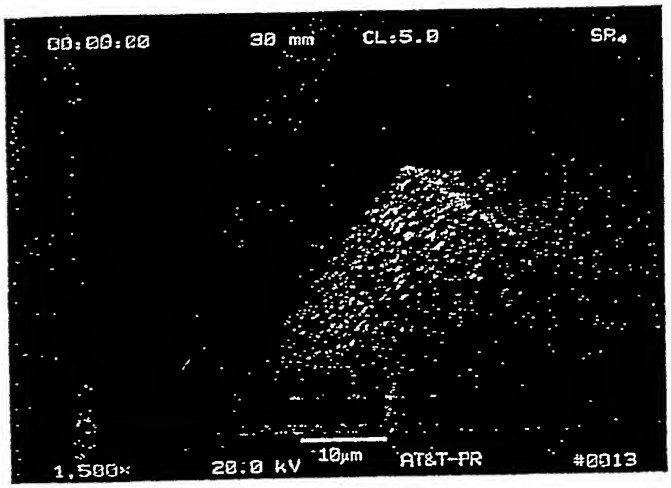

Figure 31. Bonded fiber (which is also shown in upper photomicrograph of Figure 30) shows the penetration of the fiber into the aluminum film on the angular wall.

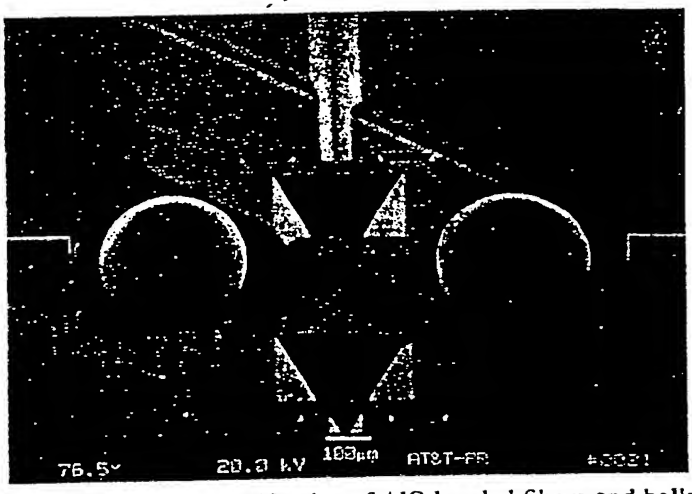

Figure 33. Higher magnification of AlO bonded fibers and balls on a silicon optical substrate shown in Figure 32.

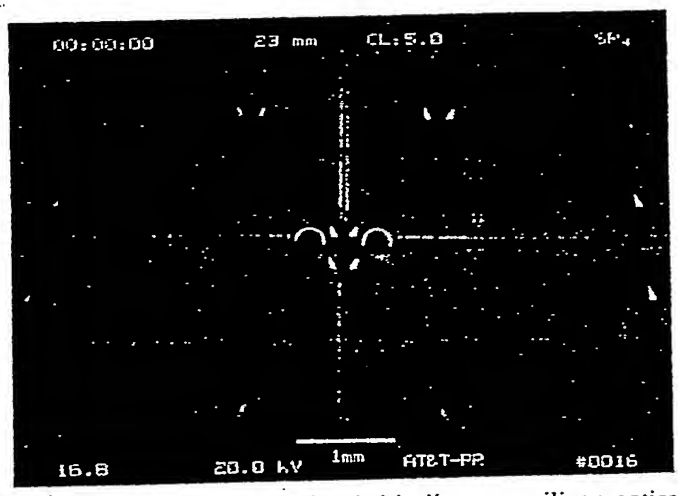

Figure 32. Fibers and balls bonded in-line on a silicon optical substrate which was used to obtain straight thru loss measurements during bonding and thermal cycling.